

Transmission properties in waveguides: An optical streamline analysis

A. S. Sanz,^{*} J. Campos-Martínez,[†] and S. Miret-Artés
Instituto de Física Fundamental (IFF-CSIC), Serrano 123, 28006 Madrid, Spain

A novel approach to study transmission through waveguides in terms of optical streamlines is presented. This theoretical framework combines the computational performance of beam propagation methods with the possibility to monitor the passage of light through the guiding medium by means of these sampler paths. In this way, not only the optical flow along the waveguide can be followed in detail, but also a fair estimate of the transmitted light (intensity) can be accounted for by counting streamline arrivals with starting points statistically distributed according to the input pulse. Furthermore, this approach allows to elucidate the mechanism leading to energy losses, namely a vortical dynamics, which can be advantageously exploited in optimal waveguide design.

OCIS Codes: 030.5260, 030.5290, 050.4865, 060.2310, 060.4230, 070.2580

I. INTRODUCTION

Optical waveguide design is central to the development of efficient devices with applications in optoelectronics and nanotechnologies [1]. More recently, it has also become relevant to quantum information processing and quantum technologies based on photons [2, 3]. Very often these designs involve a complexity that arises from the particular details of individual guiding elements as well as the existence of a network of waveguides staged in series. Thus, to ensure optimal guiding conditions, it is of interest to develop efficient and flexible propagation and optimization first-principle procedures, more specifically, implementing and developing appropriate propagation methods to solve Maxwell's equations. These vector equations are highly demanding in terms of computational effort if adequate balance in accuracy is required.

For some particular types of waveguides (e.g., optical waveguides made of semiconductor materials), though, light propagation can be properly accounted for by the scalar optics approximation, in particular, the Helmholtz equation [4–6]. In those cases where the waveguides do not bend too severely and the ratio between the inside and outside refractive indexes is relatively small, their study can be further simplified by appealing to the paraxial or small-angle approximation. The Helmholtz equation is then replaced by a simpler scalar wave equation, namely the paraxial equation [4, 5]. Of course, in more adverse cases the paraxial approximation can no longer be used and other types of approximations can be considered, such as the so-called wide angle equation [7], but this goes beyond the scope of this work.

The analogy between optical and matter waves is a well-known subject in optics [6, 8–10], which becomes more apparent when considering the isomorphism between the paraxial equation and the time-dependent Schrödinger equation. Hence, numerical methods available in quantum mechanics to propagate wave packets

[11–13] can also be used to study optimal waveguiding conditions for the transmission of light pulses [14–16] — actually, in some cases, these methods came originally from optics, which shows the fruitful interplay between these two branches of physics—, where they are known as beam propagation methods (BPMs).

Now, apart from having efficient BPMs, one of the key questions that arises in a natural way from the quantum-optical analogy is whether some extra tools can be devised and used to analyze and to better understand the transport properties inside waveguides. In this regard, consider, for example, the analysis of diffraction and interference with polarized light by means of photon trajectories [17–19], which are the direct optical analog of the quantum trajectories coming from the Bohmian formulation of quantum mechanics [20, 21]. These studies, motivated by single-photon experiments [22–24], allowed a better understanding of the flux of electromagnetic energy in such contexts, accounting for the formation of interference fringes or their disappearance depending on the polarization of the interfering beams. In fact, in spite of the theoretical nature of these studies, recently photon trajectories have been inferred from experimental evidence [25], confirming the topology of those previously reported theoretically [18].

In this work, an analogous concept to that of photon trajectory is considered within the context of waveguiding and utilized to render some light on how transport is conducted inside waveguides. Unlike the photon trajectories mentioned above, here we take advantage of the isomorphism between the paraxial equation and the time-dependent Schrödinger equation, which allows us to readily extend the Bohmian approach to the light transport accounted for by the former. Since the light flux analyzed is time-independent, to avoid possible connotations associated with the concept of photon trajectory (as describing the time-evolution of particles rather than fluxes), the concept of optical streamline will be used. These streamlines are synthesized “on the fly” in combination with the BPM used to obtain the exact evolution of the pulse inside the waveguide [14]. As it is shown, the optical streamlines provide us with an alternative, complementary insight to the standard wave approach,

^{*}Electronic address: asanz@iff.csic.es

[†]Electronic address: jcm@iff.csic.es

which allows us to understand the flow of light inside waveguides by monitoring its way through locally, i.e., just like a tracer particle allows us to determine the flow of a classical fluid. In this regard, this constitutes an interesting alternative tool to analyze this kind of systems and their optical properties. In particular, we show how optical streamlines provide us with detailed dynamical (though stationary) information about guiding properties (i.e., the transport of light) and the loss mechanism. Although there are different designs depending on their particular application, in order to properly introduce the language and methodology, here we focus on the Y-junction structure, which is widely used and appears as the main component in many other more intricate optical devices. More specifically, as a working model, the Y-junction geometry developed by Langer and co-workers [26, 27] has been considered, which is closely related to realistic waveguides of potential industrial interest.

This work is organized as follows. In Section II, a brief account on the theory behind both the paraxial equation and its connection to Bohmian mechanics is presented. Section III deals with the application of this theory to the analysis of the light flow through Y-junction-type waveguides, providing some numerical results. Finally, in Section IV the main conclusions and future perspectives are summarized.

II. THEORY

Consider the optical axis of the waveguide is oriented along the z -direction, while its transversal section is parallel to the XY -plane. Moreover, the passage of light through the waveguide is describable in terms of a time-harmonic electromagnetic field, which allows us to simplify the treatment by considering a stationary or time-independent scalar field $\Phi(\mathbf{r})$ [6]. This implies $\Phi(\mathbf{r})$ satisfies Helmholtz's equation,

$$\nabla^2\Phi + n^2k^2\Phi = 0, \quad (1)$$

plus the corresponding boundary conditions imposed by the shape and refractive properties of the waveguide. In Eq. (1), $n \equiv n(\mathbf{r})$ is the position-dependent refractive index inside the waveguide and $k = 2\pi/\lambda$, with λ being the light wavelength in vacuum.

Taking into account this configuration for the waveguide, in the small-angle or paraxial approximation, the scalar field Φ can be approximated by a plane wave along the z -direction modulated by a certain complex-valued amplitude [6], i.e.,

$$\Phi(\mathbf{r}) = \phi(\mathbf{r})e^{ik_z z}. \quad (2)$$

In other words, this means that, for this type of nonuniform waveguides, fast oscillations can be separated from slower ones. Accordingly, when moving inside the bulk, this splitting allows us to write $k_z = \beta_0 = kn_0$, where

n_0 is the *bulk index*. Substituting (2) into Helmholtz's equation (1), the latter can be recast as

$$2ik_z \frac{\partial\phi}{\partial z} + \frac{\partial^2\phi}{\partial z^2} = -\nabla_{\perp}^2\phi + (k_z^2 - k^2n^2)\phi. \quad (3)$$

Here, ∇_{\perp}^2 denotes the transverse Laplacian, i.e., the Laplacian on the subspace perpendicular to the propagation direction, $\nabla_{\perp}^2 = \partial^2/\partial x^2 + \partial^2/\partial y^2$. Apart from the paraxial approximation, if we also assume the slowly varying envelope approximation holds, i.e., the envelope ϕ varies slowly in space compared to $2\pi/k_z$, the highest-order derivative, $\partial^2\phi/\partial z^2$, can be neglected in Eq. (3), which can be expressed as

$$2i\beta_0 \frac{\partial\phi}{\partial z} = -\nabla_{\perp}^2\phi + (\beta_0^2 - k^2n^2)\phi. \quad (4)$$

As it can be readily noticed, this equation is isomorphic to the time-dependent Schrödinger equation, except for the evolution, which is not in time, but in terms of the z -coordinate (within this context the space z -coordinate acts as the “evolution” parameter). From now on, the transversal coordinates (x, y) will be denoted collectively by means of the vector \mathbf{R} . This quantum-optical analogy becomes more apparent if Eq. (4) is recast as

$$i \frac{\partial\phi}{\partial z} = \left[-\frac{1}{2kn_0} \nabla_{\perp}^2 + V(\mathbf{r}) \right] \phi, \quad (5)$$

where

$$V(\mathbf{r}) = \frac{k}{2n_0} [n_0^2 - n^2(\mathbf{r})] \quad (6)$$

is an effective potential function accounting for the waveguide refractive profile and $\mu \equiv \beta_0 = kn_0$ plays the role of an “optical mass” [28, 29]. Here, in particular, we have chosen an optical effective mass to be $\mu = 2\beta_0$ in order to enhance the dynamical effects inside the guide. Nevertheless, it is important to stress that, while Schrödinger's equation describes a true time-evolution, Eq. (5) only describes how the stationary, three-dimensional scalar field ϕ (and, therefore, the light intensity) distributes along the waveguide. The fact that this field behaves differently along the z -coordinate than along the transversal section is used conveniently from a computational viewpoint to solve the corresponding three-dimensional wave equation, but the field itself is always stationary.

Following with the quantum-optical analogy, consider ϕ is now expressed in polar form,

$$\phi(\mathbf{R}, z) = \rho^{1/2}(\mathbf{R}, z)e^{iS(\mathbf{R}, z)}, \quad (7)$$

in order to establish a parallelism with Bohmian mechanics [20, 21], also known as quantum hydrodynamics [30, 31]. Within this formulation of quantum mechanics, ρ and S denote, respectively, the probability density and phase of the wave function describing a quantum particle of mass m , both being real-valued functions. In the

present context, though, these quantities are related, respectively, to the (stationary) energy density inside the waveguide and its flux. After substitution of (7) into the optical Schrödinger-like equation (5), we obtain a system of two real coupled equations,

$$\frac{\partial \rho}{\partial z} + \nabla \cdot \mathbf{J} = 0, \quad (8)$$

$$\frac{\partial S}{\partial z} + \frac{(\nabla_{\perp} S)^2}{2\mu} + V_{\text{eff}} = 0. \quad (9)$$

Equation (8) is a continuity equation, which describes how the energy is distributed throughout the waveguide. However, given the parametrization in terms of z , this equation can also be interpreted as accounting for the connection between the energy distribution $\rho = \phi^* \phi$ along the transversal section at a certain value of z with its flux through this section, \mathbf{J} . This flux can be expressed as $\mathbf{J} = \rho \mathbf{v}$, i.e., in terms of a local velocity field,

$$\mathbf{v} = \frac{\nabla_{\perp} S}{\mu} = \frac{\hbar}{2\mu i} \left(\frac{\phi^* \nabla_{\perp} \phi - \phi \nabla_{\perp} \phi^*}{\phi^* \phi} \right). \quad (10)$$

Assuming $\mathbf{v} = \mathbf{R}' = d\mathbf{R}/dz$ and then integrating for x and y along the time-like z -coordinate with different initial conditions, one obtains a series of optical streamlines. These streamlines allow us to visualize how energy flows inside the guide at a local level. That is, we can connect causally a particular point of the input pulse with another one of the output one in a non-ambiguous fashion —unlike classical rays, the optical streamlines evolve in space in accordance with the wave-like behavior of the field ϕ . In quantum mechanics the corresponding quantum streamlines monitor the flow described by the quantum (probabilistic) fluid and have been used earlier in the literature to describe different physical systems [32–36] as well as to devise new numerical propagation schemes [37].

In order to better understand the meaning of two points being causally connected, we need to focus on Eq. (9). This equation describes the evolution (in terms of the z -coordinate) of the phase field S along the waveguide and presents the form of a quantum Hamilton-Jacobi equation [20, 21]. In it, the effective potential V_{eff} consists of two contributions, the potential V defined above [see Eq. (6)] and a kind of “optical” potential,

$$Q \equiv -\frac{1}{2\mu} \frac{\nabla^2 \rho^{1/2}}{\rho^{1/2}} = \frac{1}{4\mu} \left[\frac{1}{2} \left(\frac{\nabla \rho}{\rho} \right)^2 - \frac{\nabla^2 \rho}{\rho} \right], \quad (11)$$

which is analogous to the *quantum potential* of Bohmian mechanics. As in the classical version of the Hamilton-Jacobi mechanics, solutions of Eq. (9) define trajectories as the perpendicular streamlines to surfaces of constant phase S , which here translates into the equation of motion (10). The coupling between (8) and (9) through Q (or, equivalently, ρ and its space derivatives) is the reason why the wave formulation for waveguides differs from its

geometric counterpart. The guidance condition (10) thus allows to properly include typical wave-like features like interference and diffraction, for example, in the topology of the streamlines, which does not happen, however, in the rays one obtains from geometric optics.

III. NUMERICAL RESULTS

A. The waveguide design

Consider a waveguide that transports a light beam injected at $z = 0$ to a given distance $z = L$. Apart from its particular geometry, the transport properties of this waveguide are characterized by the bulk refractive index (n_0), the guide refractive index (n_1), and the cladding refractive index (n_2). Physically, these refractive indexes can be associated with an effective potential function that accounts for the waveguide refractive profile (the profile along the transversal direction), as seen in the previous section. Inside the waveguide this effective potential or refractive profile reads as

$$V = \frac{k}{2n_0} (n_0^2 - n_1^2), \quad (12)$$

while outside it is given by

$$V = \frac{k}{2n_0} (n_0^2 - n_2^2). \quad (13)$$

In order to simplify our study, but without loss of generality, we are also going to assume that the electric field depends only on one of the two transversal coordinates, say x . This is the condition that determines the confinement of light inside the waveguide [6]. The other direction, y , will be less relevant, only adding some attenuation when moving further away inside the bulk. Thus, in the present case, the distribution of light inside the waveguide is accounted for by a stationary (time-independent) scalar field $\phi(x, z)$. Alternatively, taking into account the wave picture described in the previous section, ϕ can also be interpreted as describing the evolution of a pulse of light distributed along the x (space-like) direction as the value of z (time-like) coordinate increases.

The configuration of the waveguide along the z -direction is as displayed in Fig. 1. It is a Y-junction which utilizes a 1×2 multimode interference (MMI) device with a lowered refractive index (n_w) in the junction or wedge region, as proposed by Langer *et al.* [27] (here, though, we have assumed the wedge refractive index to be equal to the guide one). This wedge reduces the losses over a rather large range of Y-junction angles. Details on the numerical values for the geometric and refractive index parameters considered here are given in Table I.

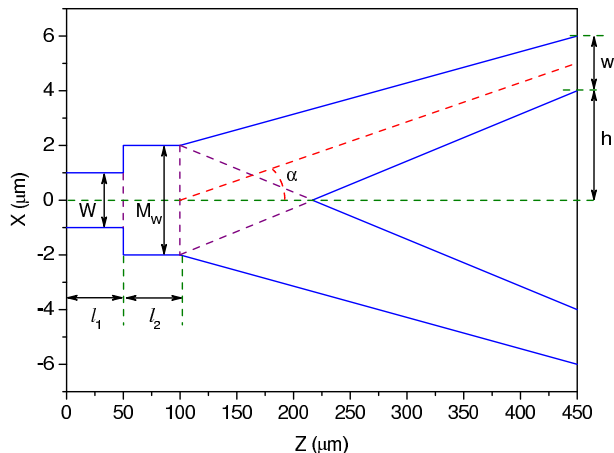


FIG. 1: Geometrical layout of the Y-junction design considered here, where the significant (geometrical) parameters are also displayed (see Table I).

B. Numerical methodology

In this work, the Schrödinger-like form of the paraxial equation, Eq. (5), has been solved by taking advantage of the computational machinery developed in standard quantum wave-packet propagations to solve the time-dependent Schrödinger equation. More specifically, we have considered the split-operator technique combined with the fast Fourier transform method [11–13]. As it has been shown [14, 15], this type of BPM results very efficient computationally, particularly in optimal control scenarios.

As mentioned above, the purpose of this work is to combine the computational performance of BPMs with

TABLE I: Values of the different parameters considered in the design of the waveguide used in the calculations shown here (see text for details).

Parameter	
λ (μm)	1
W (μm)	2
M_W (μm)	4
ℓ_1 (μm)	50
ℓ_2 (μm)	100
h (μm)	4
w (μm)	2
α	$\sim 0.82^\circ$
n_0	3.558
n_1	3.568
n_2	3.558
n_w	3.568

the physical insight provided by the optical streamlines. Therefore, regarding the calculation of the optical streamlines, we have chosen to solve Eq. (10) “on the fly”, i.e., once ϕ has been evolved from z to $z + \delta z$, the streamline is updated, from $x(z)$ to $x(z + \delta z)$, by means of a fourth-order Runge-Kutta integrator fed with the field ϕ , according to the last equality in (10). This is a method that has been previously applied to the study of matter-wave diffraction by periodic gratings [38]. Nevertheless, from a merely computational point of view, one could also consider any of the so-called quantum trajectory methods [37], based on solving also “on the fly” Eqs. (8), (9) and (10), which would skip solving the paraxial equation.

Once the method is set up, another important element when dealing with optical streamlines is that, in order to obtain a good representation of the pulse at each value of the z -coordinate, one needs to have an optimal sampling of the initial pulse, namely $\rho(x, 0)$. Since one of the purposes here is to show that the evolution of the pulse along the waveguide can be followed by looking at the density of streamlines rather than monitoring ϕ itself, we have not optimized the number of streamlines considered. Thus, a total of 11,256 initial positions $x_0 = x(z = 0)$ have been randomly generated according to the weight $\rho(x, 0)$ [39]. This sampling has been made in such a way that the value of $\rho(x_0, 0)$ was confined between the maximum of the intensity distribution (here, at $x = 0$) and 10^{-3} times this value, i.e., $\rho(x = 0, 0) \geq \rho(x_0, 0) \geq 10^{-3} \times \rho(x = 0, 0)$, for all x_0 [see Fig. 2(a)]. These initial conditions have then been propagated and, at each value of z , a histogram was built up with them to compare with the intensity obtained from the paraxial equation. This step in the calculation is crucial in order to obtain a fair reproduction of the optical result. We have observed that the calculation of the streamlines “on the fly”, as described above, does not decrease much the efficiency of the BPM considered when computing a low number of sampler streamlines, i.e., streamlines calculated to determine the flux of light without caring much about having a good sampling. Otherwise, the time of computation increases *strictly* linearly with the number of streamlines, as in any standard trajectory calculation.

C. Analysis of the results

In Fig. 2(a), it is observed how the histogram fairly reproduces the profile (along the waveguide transversal section) of the input pulse at $z = 0 \mu\text{m}$. The same is also found for larger values of the z -coordinate, at $z = 450 \mu\text{m}$, as seen in Fig. 2(b). In general, this behavior can be found at any value of z , which allows us to study the transmission properties along the waveguide by only considering the propagation of the histogram, as shown in Fig. 3. In this plot, the intensity reaches a maximum as soon as it leaves the 1×2 MMI device and then splits up into two identical fluxes, each one displaying a series of bounces inside its corresponding waveguide as they

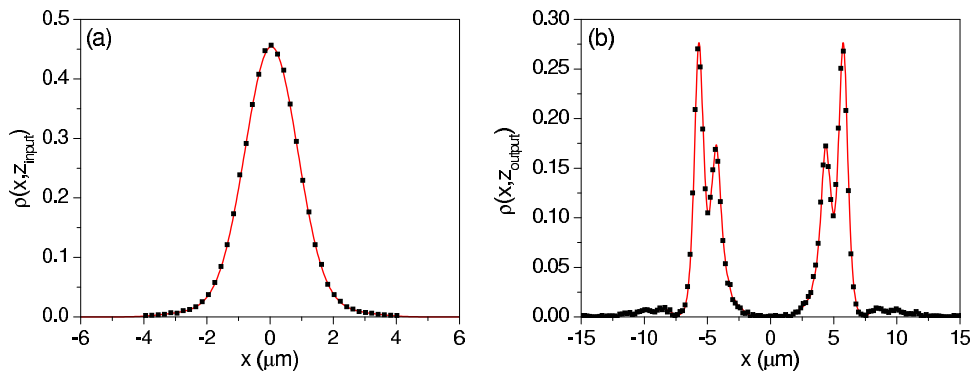


FIG. 2: Initial (a) and final (b) intensity transmitted through the waveguide. In each panel, black squares denote the optical streamline calculation (histogram), while the red solid accounts for the value obtained from the standard optical calculation (paraxial equation). The parameters used in these calculations are given in Table I.

propagate. These bounces can be somehow related to the bounces that a light ray would undergo according to a geometrical optical viewpoint (the ray propagates along a straight line until it reaches the boundary of the waveguide, which defines its turning point in accordance with the laws of reflection and refraction).

The analogy with geometrical rays can be extended by means of the optical streamlines here defined. In Fig. 4, a set of 200 of such streamlines, chosen (in proportion) from among the full set run, are plotted. As it can be noticed, optical streamlines behave as geometrical rays, undergoing a series of bounces and reflection at the boundaries of the waveguide, although their flow is more laminar, like tracer particles moving on a fluid. This is a consequence of the fact that they follow a wave and therefore they have to accommodate to the features undergone by such a wave, such as diffraction, interference or refraction. In connection with this property, also note that they satisfy the non-crossing property of Bohmian trajectories [40]: two streamlines cannot pass through the same position x for the same value of the evolution coordinate, z . This allows us to establish a clear difference between streamlines evolving along the two branches of the Y-junction. In the case considered here, this might seem to be not so important, for the evolution along z is symmetric with respect to $x = 0$. However, notice that as soon as a slight asymmetry between pathways would appear (different refractive index, length, shape, etc.), the splitting would also be different. In such a case, the optical streamlines will provide us with unambiguous information on which specific portion of the input signal goes through each branch. Thus, this type of information, which cannot be disentangled in wave-based treatments by their intrinsically global nature, can be of interest in applications based on waveguide technologies, such as Mach-Zehnder interferometry or other optical interference devices. Actually, even in the present case, this property results useful, because it allows us to causally connect [41] a certain feature from the output signal at $z = 450 \mu\text{m}$ with a particular region of the in-

put, at $z = 0$. Later on this information can be used to make the sampling only over a certain subset of initial conditions (e.g., those that does not lead to losses at $z = 450 \mu\text{m}$).

Apart from the properties above, an additional interesting feature enabled by an analysis based on optical streamlines is the detection of energy losses through the waveguide boundaries. Detection of such losses by standard means, i.e., by only studying the evolution of $\phi(x, z)$, the intensity $\rho(x, z)$ needs to be integrated over

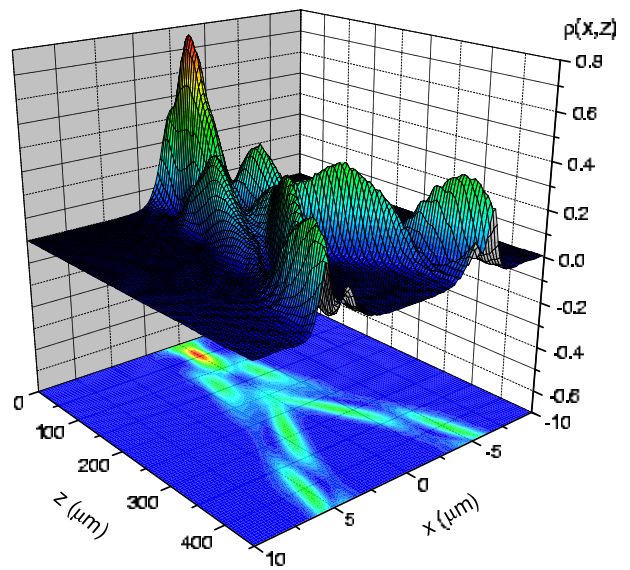


FIG. 3: Three-dimensional representation showing the evolution of the initial pulse $\rho(x,0)$ as it propagates (along the z -coordinate) throughout the waveguide (below, the corresponding contour-plot is also displayed). In particular, $\rho(x, z)$ has been obtained as a histogram-like distribution of optical streamlines at each z value, which corresponds fairly well with the representation one would find by standard wave propagation methods (see text for details). The parameters used in these calculations are given in Table I.

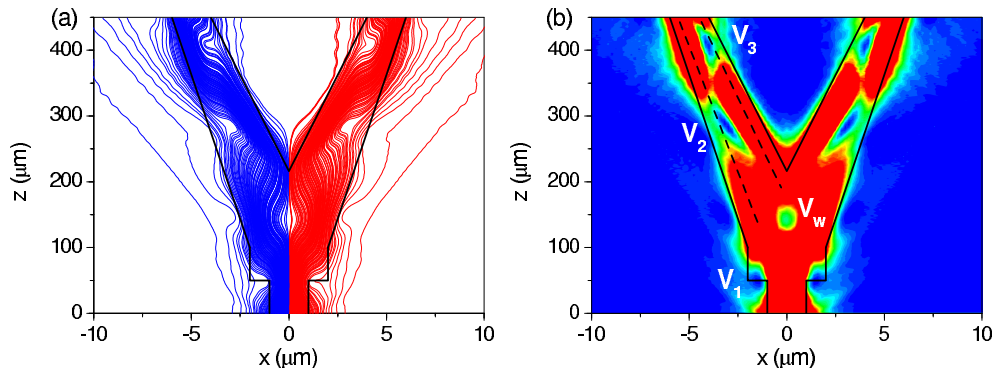


FIG. 4: Optical streamlines (a) and contour-plot of the evolution of the histogram (b) illustrating the flow of light throughout the waveguide. In both figures, the straight black lines mark the waveguide boundaries (see Fig. 1). In part (a), blue and red lines are used to emphasize the fact optical streamlines also satisfy the non-crossing rule that characterizes both quantum [40] and optical fluxes [18]. In part (b), the maximum value of the contours is set up to 0.1 in order to appreciate the outgoing light flow. White labels correspond to different vortices that appear during the evolution of the flow (see text for details).

the waveguide cross-section (at a given z value). From a more graphical viewpoint, the intensity should be enlarged until the amount of intensity that is flowing outside is perceived [see Fig. 4(b)]. For example, in Fig. 2(b) the presence of two “wings” lying out of the waveguide boundaries is clearly seen, which indicate the leakage of light from the waveguide. However, they are neither perceived in the contour-plot of Fig. 3, nor the continuous outwards flow of energy (or how and when this flow happens). A more convenient and insightful way to understand this flow arises by observing the topology of the optical streamlines, as it is apparent from Fig. 4(a). Although the outermost streamlines are associated with very low intensity (that is precisely the reason why they appear so sparse in the figure), it is readily noticed how the flow is outwards. Actually, whenever a node of the intensity appears, it pushes away the streamlines, as can be seen at $z \approx 150 \mu\text{m}$, $275 \mu\text{m}$ or $450 \mu\text{m}$ (and inwardly at $z \approx 400 \mu\text{m}$). In this sense, optical streamlines acquire the role of optical tracers of the energy flow inside the waveguide, allowing us to monitor it at each step. This property thus results very useful in the optimal design of waveguides and the control of light inside them, for it gives us a straightforward method to test losses and gains.

At a more detailed level of description, the optical streamlines provide us with a better understanding on the dynamics that is taking place inside the waveguide, such as the different features which one can observe later on in the modes or energy losses. In this regard, consider first the high intensity peak observed at the entrance of the second section of the 1×2 MMI (see Fig. 3), which later on gives rise to a node or vortex [V_w , in Fig. 4(b)] in the wedge center. By inspecting the optical streamlines [see Fig. 4(a)], one readily notices how most of them quickly undergo an inwards motion as z increases, just before V_w becomes incipient at the position where the second section of the 1×2 MMI starts (regarding the streamlines that surmount the vortex through the op-

posite side; see comments below). By construction, the tight squeezing of the swarm of streamlines takes place just at the entrance of the second section of the 1×2 MMI, from which it undergoes a fast expansion. This expansion causes the splitting of the beam into two distinctive halves (partial beams), each one channeled into one of the branch of the Y-junction and, moreover, a vortex in between. It is interesting to compare this behavior to that of a classical fluid which is released from a pipe, thus giving rise to channeled streams and hollows or low density regions in between.

Now, consider only one of the branches of the waveguide, for example, the left-hand side one. From a simple inspection of Fig. 4(b), where the contours refer to low intensity values (up to 10% of its maximum, at the entrance of second section of the 1×2 MMI; see Fig. 3), one observes that the flow of energy appears and disappears alternatively along two pathways as z increases (see black dashed lines). This is an effect of the modes generated within the branches of the waveguide that can be easily explained in terms of a simple model. Consider that two kind of wave packets travel along each pathway. They are being populated alternatively as they evolve along z , i.e., when one starts to gain population, the other loses it, just as in a simple two-level system,

$$\phi(x, z) = \cos(\omega z)\varphi_1(x) + \sin(\omega z)\varphi_2(x). \quad (14)$$

According to this simple model one can easily explain that, for example, near the vortex V_2 [see Fig. 4(b)], one of the pathways starts to get depopulated very quickly, while the other reaches its maximum (see also Fig. 3). The same behavior is again observed when approaching V_3 . However, although this two-level model describes the features in the population changes as the optical modes travel through the waveguide branches, no information is provided about the population transfer between pathways or energy losses. These are processes suitable to be explained by means of the associated optical streamlines,

for they provide us with precise information about the energy flux and its evolution along the waveguide, as seen above. Thus, as it can be seen as the mode approaches V_2 [see Fig. 4(a)], the streamlines start to move smoothly rightwards, from one pathway to the other, until their number has decreased considerably in the first pathway. Near V_2 there are three options for those streamlines still remaining along the first pathway: (1) some of them undergo a sudden turn and will enter into the second pathway stream, (2) some will slightly bend and will continue along the first pathway beyond the vortex, and (3) another group leave the waveguide after the bending, thus giving rise to the losses (eventually, streamlines from group 2 will also scape). This behavior can be observed not only around V_2 , but around any other external vortex (V_1 , V_3 and the homologous vortices along the second pathway), i.e., any vortex facing the boundaries of the waveguide. The goal of waveguide optimal design is to avoid losses and therefore it can highly benefit from this optical streamline representations.

IV. SUMMARY AND FUTURE PERSPECTIVES

The purpose here was to introduce the concept of optical streamline in the literature of waveguides as an analytical tool, in combination with efficient BPMs to carry out their propagation. To carry out our hydrodynamical analysis, we have considered as a working model a Y-junction with a geometry closely related to realistic waveguides of potential industrial interest, originally proposed some year ago within the broad family of Y-junctions [27]. The particularity of these devices is that

their design seeks for a minimum loss of the input while having a clean splitting of the signal, at the same time. Thus, given the interest and relevance of these designs in modern technologies, to have at our disposal additional tools which can help us to design, study, explain and understand such systems is of great importance. In this regard, here we have mainly focused on determining how the modes travel through the wave as well as on elucidating the energy/light loss mechanism in waveguides. These two features can be efficiently controlled by means of an appropriate design [15, 26], which is precisely the scope of the waveguide optimal design techniques and the eventual target of our optical streamline analysis, where it can be of much interest and help. This is actually a natural and important extension of the present work, which is currently under development. Nonetheless, we also like to stress the general usefulness of the proposed new tool, which might be of relevance in other more complex scenarios where interference or merging of different signals could be more efficiently studied (e.g., Mach-Zehnder interferometers [15]), as well as other domains going beyond the paraxial approximation (e.g., the wide-angle equation [7]).

Acknowledgments

This work has been supported by the Ministerio de Economía y Competitividad (Spain) under Projects FIS2010-22064-C02-02, FIS2010-18132 and FIS2010-22082, as well as by the COST Action MP1006 (*Fundamental Problems in Quantum Physics*). A. S. Sanz would also like to thank the Ministerio de Economía y Competitividad for a “Ramón y Cajal” Research Fellowship.

-
- [1] J. S. Volker, Y. Ziliang, F. Rupert, W. Yuan, B. Guy, Y. Xiaobo, and Z. Xiang, “Experimental demonstration of low-loss optical waveguiding at deep sub-wavelength scales,” *Nat. Commun.* **2**:331 doi: 10.1038/ncomms1315 (2011).
 - [2] A. Politi, M. J. Cryan, J. G. Rarity, S. Yu, and J. L. O’Brien, “Silica-on-silicon waveguide quantum circuits,” *Science* **320**, 646–649 (2008).
 - [3] L. Sansoni, F. Sciarrino, G. Vallone, P. Mataloni, A. Crespi, R. Ramponi, and R. Osellame, “Polarization entangled state measurement on a chip,” *Phys. Rev. Lett.* **105**, 200503(1–4) (2010).
 - [4] S. Banerjee and A. Sharma, “Propagation characteristic of optical waveguiding structures by direct solution of the Helmholtz equation for total fields,” *J. Opt. Soc. Am. A* **6**, 1884–1894 (1989).
 - [5] R. Scarmozzino, A. Gopinath, R. Pregla, and S. Herlert, “Numerical techniques for modeling guided-wave photonic devices,” *J. Opt. Soc. Am. A* **6**, 150–162 (2000).
 - [6] M. Born and E. Wolf, *Principles of Optics. Electromagnetic Theory of Propagation, Interference and Diffraction of Light* (Cambridge University Press, Cambridge, 1999), 7th ed.
 - [7] J. Campos-Martínez and R. D. Coalson, “The wide-angle equation and its solution through the short-time iterative lanczos method,” *Appl. Opt.* **42**, 1732–1742 (2003).
 - [8] H. A. Buchdahl, *An Introduction to Hamiltonian Optics* (Cambridge University Press, Cambridge, 1970).
 - [9] D. Gloge and D. Marcuse, “Formal quantum theory of light rays,” *J. Opt. Soc. Am.* **59**, 1629–1631 (1969).
 - [10] W. K. Kahn and S. Yang, “Hamiltonian analysis of beams in an optical slab guide,” *J. Opt. Soc. Am.* **73**, 684–690 (1983).
 - [11] M. D. Feit, J. J. A. Fleck, and A. Stieger, “Solution of the Schrödinger equation by a spectral method,” *J. Comput. Phys.* **47**, 412–433 (1982).
 - [12] M. D. Feit and J. J. A. Fleck, “Solution of the schrödinger equation by a spectral method II: Vibrational energy levels of triatomic molecules,” *J. Chem. Phys.* **78**, 301–308 (1983).
 - [13] C. Leforestier, R. H. Bisseling, C. Cerjan, M. D. Feit, R. Friesner, A. Guldberg, A. Hammerich, G. Jolicard, W. Karrlein, H.-D. Meyer, N. Lipkin, O. Roncero, and R. Kosloff, “A comparison of different propagation schemes for the time dependent Schrödinger equation,” *J. Comp. Phys.* **94**, 59–80 (1991).

- [14] D. K. Pant, R. D. Coalson, M. I. Hernández, and J. Campos-Martínez, “Optimal control theory for the design of optical waveguides,” *J. Light. Tech.* **16**, 292–300 (1998).
- [15] D. K. Pant, R. D. Coalson, M. I. Hernández, and J. Campos-Martínez, “Optimal control theory for optical waveguide design: Application to Y-branch structures,” *Appl. Opt.* **38**, 3917–3923 (1999).
- [16] S. Longhi, D. Janner, M. Marano, and P. Laporta, “Quantum-mechanical analogy of beam propagation in waveguides with a bent axis: Dynamic-model stabilization and radiation-loss suppression,” *Phys. Rev. E* **67**, 036601(1–9) (2003).
- [17] M. Davidović, A. S. Sanz, D. Arsenović, M. Božić, and S. Miret-Artés, “Electromagnetic energy flow lines as possible paths of photons,” *Phys. Scr.* **T135**, 014009(1–5) (2009).
- [18] A. S. Sanz, M. Davidović, M. Božić, and S. Miret-Artés, “Understanding interference experiments with polarized light through photon trajectories,” *Ann. Phys.* **325**, 763–784 (2010).
- [19] M. Božić, M. Davidović, T. L. Dimitrova, S. Miret-Artés, A. S. Sanz, and A. Weis, “Generalized Arago-Fresnel laws: The eme-flow-line description,” *J. Russ. Laser Res.* **31**, 117–128 (2010).
- [20] D. Bohm, “A suggested interpretation of the quantum theory in terms of “hidden” variables. I,” *Phys. Rev.* **85**, 166–179 (1952).
- [21] P. R. Holland, *The Quantum Theory of Motion* (Cambridge University Press, Cambridge, 1993).
- [22] T. L. Dimitrova and A. Weis, “The wave-particle duality of light: A demonstration experiment,” *Am. J. Phys.* **76**, 137–142 (2008).
- [23] T. L. Dimitrova and A. Weis, “Lecture demonstrations of interference and quantum erasing with single photons,” *Phys. Scr.* **T135**, 014003(1–4) (2009).
- [24] T. L. Dimitrova and A. Weis, “Single photon quantum erasing: A demonstration experiment,” *Eur. J. Phys.* **31**, 625–637 (2010).
- [25] S. Kocsis, B. Braverman, S. Ravets, M. J. Stevens, R. P. Mirin, L. K. Shalm, and A. M. Steinberg, “Observing the average trajectories of single photons in a two-slit interferometer,” *Science* **332**, 1170–1173 (2011).
- [26] R. D. Coalson, D. K. Pant, A. Ali, and D. W. Langer, “Computing the eigenmodes of lossy field-induced optical waveguides,” *J. Light. Tech.* **12**, 1015–1022 (1994).
- [27] D.-S. Min, D. W. Langer, D. K. Pant, and R. D. Coalson, “Numerical techniques for modeling guided-wave photonic devices,” *Fiber Integr. Opt.* **16**, 331–342 (1997).
- [28] P. K. Tien, “Integrated optics and new wave phenomena in optical waveguides,” *Rev. Mod. Phys.* **49**, 361–420 (1981).
- [29] P. K. Tien, “Rules of refractive index and a potential well model of the optical waveguides,” *Radio Sci.* **16**, 437–444 (1981).
- [30] E. Madelung, “Quantentheorie in hydrodynamischer Form,” *Z. Phys.* **40**, 322–326 (1926).
- [31] I. Bialynicki-Birula, M. Cieplak, and J. Kaminski, *Theory of Quanta* (Oxford University Press, Oxford, 1992).
- [32] I. Bialynicki-Birula and Z. Bialynicka-Birula, “Magnetic monopoles in the hydrodynamic formulation of quantum mechanics,” *Phys. Rev. D* **3**, 2410–2412 (1971).
- [33] J. O. Hirschfelder, A. C. Christoph, and W. E. Palke, “Quantum mechanical streamlines. I. square potential barrier,” *J. Chem. Phys.* **61**, 5435–5455 (1974).
- [34] J. O. Hirschfelder, C. J. Goebel, and L. W. Bruch, “Quantized vortices around wavefunction nodes. II,” *J. Chem. Phys.* **61**, 5456–5459 (1974).
- [35] J. O. Hirschfelder and K. T. Tang, “Quantum mechanical streamlines. III. idealized reactive atom-diatom molecule collision,” *J. Chem. Phys.* **64**, 760–785 (1976).
- [36] J. O. Hirschfelder and K. T. Tang, “Quantum mechanical streamlines. IV. collision of two sphere with square potential wells or barriers,” *J. Chem. Phys.* **65**, 470–486 (1976).
- [37] R. E. Wyatt, *Quantum Dynamics with Trajectories* (Springer, New York, 2005).
- [38] A. S. Sanz, F. Borondo, and S. Miret-Artés, “Particle diffraction studied using quantum trajectories,” *J. Phys.: Condens. Matter* **14**, 6109–6145 (2002).
- [39] A. S. Sanz, D. López-Durán, and T. González-Lezana, “Investigating transition state resonances in the time domain by means of bohmian mechanics: The F+HD reaction,” *Chem. Phys.*, doi:10.1016/j.chemphys.2011.07.017 (posted 24 July 2011, in press).
- [40] A. S. Sanz and S. Miret-Artés, “A trajectory-based understanding of quantum interference,” *J. Phys. A: Math. Theor.* **41**, 435303(1–23) (2008).
- [41] A. S. Sanz and S. Miret-Artés, “Determining final probabilities directly from the initial state,” <http://arxiv.org/abs/1112.3830>.